Performance Evaluation of the CNAV Broadcast Ephemeris

Ahao Wang[1,2], Junping Chen[2,3,4], Yize Zhang[2,5], Jiexian Wang[1] and Bin Wang[2]

[1](*College of Surveying and Geo-Informatics, Tong ji University, Shanghai 200092, China*)
[2](*Shanghai Astronomical Observatory, Chinese Academy of Sciences, Shanghai 200030, China*)
[3](*School of Astronomy and Space Science, University of Chinese Academy of Sciences, Beijing 100049, China*)
[4](*Shanghai Key Laboratory of Space Navigation and Positioning Techniques, Shanghai Astronomical Observatory, Chinese Academy of Sciences, Shanghai 200030, China*)
[5](*Tokyo University of Marine Science and Technology, Tokyo, 1358533, Japan*)
(E-mail: junping@shao.ac.cn)

The new Global Positioning System (GPS) Civil Navigation Message (CNAV) has been transmitted by Block IIR-M and Block IIF satellites since April 2014, both on the L2C and L5 signals. Compared to the Legacy Navigation Message (LNAV), the CNAV message provides six additional parameters (two orbit parameters and four Inter-Signal Correction (ISC) parameters) for prospective civil users. Using the precise products of the International Global Navigation Satellite System Service (IGS), we evaluate the precision of satellite orbit, clock and ISCs of the CNAV. Additionally, the contribution of the six new parameters to GPS Single Point Positioning (SPP) is analysed using data from 22 selected Multi-Global Navigation Satellite System Experiment (MGEX) stations from a 30-day period. The results indicate that the CNAV/LNAV Signal-In-Space Range Error (SISRE) and orbit-only SISRE from January 2016 to March 2018 is of 0·5 m and 0·3 m respectively, which is improved in comparison with the results from an earlier period. The ISC precision of L1 Coarse/Acquisition (C/A) is better than 0·1 ns, and those of L2C and L5Q5 are about 0·4 ns. Remarkably, ISC correction has little effect on the single-frequency SPP for GPS users using civil signals (for example, L1C, L2C), whereas dual-frequency SPP with the consideration of ISCs results have an accuracy improvement of 18·6%, which is comparable with positioning accuracy based on an ionosphere-free combination of the L1P (Y) and L2P (Y) signals.

1. INTRODUCTION. As key parameters of the Global Positioning System (GPS) broadcast ephemeris, satellite orbit and clock quality directly affect stand-alone real-time

positioning applications (Hofmann-Wellenhof et al., 2008). Warren and Raquet (2003) conducted a long-term statistical analysis of GPS broadcast ephemeris orbit accuracy from 1993 to 2002 and found that its accuracy had increased year by year. Thanks to the successful implementation of the Legacy Accuracy Improvement Initiative (L-AII), which expanded the GPS monitoring network by adding tracking stations of the National Geospatial-Intelligence Agency (NGA), the GPS broadcast ephemeris accuracy has been significantly improved and the SISRE was reduced to 1·0 m in 2005 (Creel et al., 2007). Cohenour and Van Graas (2011) and Heng et al. (2011) evaluated the performance of the new GPS navigation message for Block IIR and Block IIR-M satellites launched between 2005 and 2010, showing smaller SISREs than Block IIA satellites. With the continuing replacement of old Block IIA satellites by new generation satellites (for example, Block IIR-M and Block IIF), the mean SISRE of the GPS constellation was about 0·7 m over the period 2012–2013 (Montenbruck et al., 2015).

The above studies on the accuracy of GPS broadcast ephemeris are all based on the Legacy Navigation Message (LNAV), which has been transmitted on the L1 Coarse/Acquisition (C/A) signal since the first operation of GPS. As part of the modernisation of GPS, a new civil signal (L2C) is now transmitted on the L2 frequency for Block IIR-M satellites. Two more signals (L5I5 and L5Q5) on a new frequency (L5) were also introduced as standard signals with Block IIF satellites from 2010. Meanwhile, the GPS Civil Navigation Message (CNAV), a new GPS broadcast ephemeris, was introduced, aimed at providing more flexibility and higher precision of the GPS ephemeris on the L2 and L5 bands for civilian use and has been in service since 2014 (Montenbruck et al., 2013). Compared with LNAV, there are three main differences: encoding mechanisms, message structures and parameter representations, where two orbit parameters (change rate for the semi-major axis and the mean motion) and four Inter-Signal Correction (ISC) parameters are encoded (IS-GPS-200H, 2014; IS-GPS-705D, 2014; Yin et al., 2014). The ISC parameters represent the discrepancy of L1C/A, L2C, L5I5 and L5Q5 signals with respect to the L1P(Y) signal. An initial CNAV test campaign was conducted from 15 June 2013 and obtained a SISRE of 0·58 m and 0·48 m for CNAV and LNAV, respectively (Montenbruck et al., 2015). The International Global Navigation Satellite System Service (IGS) started providing daily CNAV + LNAV broadcast ephemerides in a preliminary Recevier Independent Exchange Format (RINEX)-style format as part of the Multi-Global Navigation Satellite System (GNSS) Experiment (MGEX) brdxddd0.yyx product (where ddd and yy represents the day of year and two-digit year, respectively) from 28 April 2014 (Steigenberger et al., 2015). Steigenberger et al. (2015) assessed the performance of CNAV broadcast ephemerides from April 2014 to January 2015 with a SISRE of about 0·6 m, which is essentially identical to the LNAV SISRE for the same satellites. For the evaluation of the ISCs, Steigenberger et al. (2015) indicated that the precision of L1C/A ISC for 15 early GPS satellites is about 0·2 ns, and those of Timing Group Delay (TGD), L2C ISC and L5Q5 ISC are about 0·5 ns. For the evaluation of the influence of ISCs on Single Point Positioning (SPP), current studies either use limited data or ignore the influence of ISCs on dual-frequency positioning (Steigenberger et al., 2015; Wang et al., 2016a).

Since 2015, the number of GPS satellites providing CNAV has gradually increased from 11 to 19, which enables a global stand-alone service. Few studies on the accuracy of CNAV broadcast ephemerides for four new Block IIF (Space Vehicle Number, SVN G070 ∼ 073) satellites have been published. In this paper, we perform an evaluation of CNAV global stand-alone performance, including SISRE, ISCs and SPP. Section 2 presents the accuracy

of CNAV and LNAV broadcast ephemerides for the 19 GPS satellites between January 2016 and March 2018; Section 3 presents the performance of TGD and four ISC parameters, and these parameters are compared with Differential Code Bias (DCB) products of different organisations; Section 4 evaluates the positioning accuracy of GPS SPP based on LNAV-only, CNAV-only and CNAV + ISC; Section 5 summarises the main points of this paper.

2. CNAV/LNAV ORBIT AND CLOCK QUALITY.

2.1. *Evaluation methods.*   Compared with LNAV, CNAV provides extended orbit parameterisation including a change rate for the semi-major axis ΔA and the mean motion $\Delta \dot{n}_A$, in addition, four ISC parameters representing differences of L1C/A, L2C, L5I5 and L5Q5 signals with respect to the L1P(Y) signal are proposed in CNAV for civil user positioning (Wang et al., 2014; Steigenberger et al., 2015; Wang et al., 2016a; Du et al., 2017).

At present, the accuracy of GPS precise orbit and clock products provided by the IGS analysis centres is at the 2–3 cm level (Montenbruck et al., 2015), which can be adopted as a reference to evaluate the accuracy of broadcast ephemeris for LNAV and CNAV. To remove temporal/spatial reference discrepancies between broadcast ephemeris and precise products, some key points should be taken into account. (1) The precise ephemeris of the IGS is under the International Terrestrial Reference System (ITRF) framework, while the broadcast ephemeris uses the World Geodetic System-84 (WGS-84) coordinate system. The deviation between the two systems is about 1–2 cm; compared with broadcast ephemeris error, it is much smaller and can be neglected in comparison (Petit and Luzum, 2010). (2) Clock offset values of precise and broadcast ephemerides cannot be compared directly due to differences in the underlying realisation of the GNSS-specific system time scales. These differences affect all GPS satellites in the same manner and produce a systematic bias that may vary from epoch to epoch. In order to eliminate this bias, an ensemble clock difference is generally computed at each epoch from the average broadcast-minus-precise clock values of satellites in a constellation, and then the individual clock offset differences are corrected for this ensemble average. However, to account for avoiding the influence of a few satellites' clock gross error, we chose this ensemble median as a systematic bias (Montenbruck et al., 2015; Zhang et al., 2016). (3) The GPS precise ephemerides refer to the Centre-of-Mass (CoM) of the satellites whereas the broadcast ephemerides of all constellations directly provide the mean antenna phase centre location in the Earth fixed reference frame, which requires a proper antenna offset correction by using the empirically derived satellite antenna z-offsets in Montenbruck et al. (2018) and "ATX" (for example, igs08.atx and igs14.atx) antenna models (Schmid et al., 2007; Montenbruck et al., 2015; Zhang et al., 2016; Montenbruck et al., 2018).

SISRE is a key performance indicator, which describes the statistical uncertainty of the modelled pseudorange due to errors in the broadcast ephemeris (Montenbruck et al., 2018). The orbit-only contribution to the signal-in-space range error can be described as follows:

$$SISRE(orb) = \sqrt{(\alpha g R)^2 + \beta g(A^2 + C^2)} \tag{1}$$

The combined orbit and clock SISRE is obtained from Equation (2):

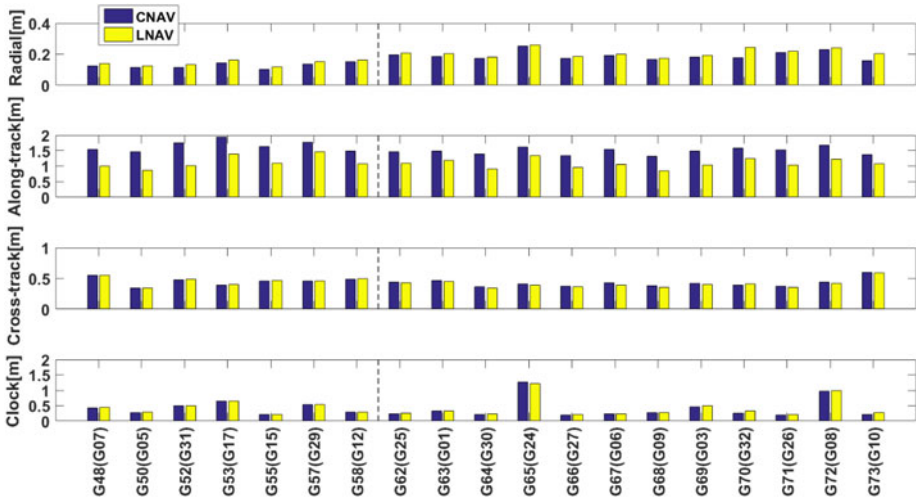$$SISRE = \sqrt{(\alpha g R - Clk)^2 + \beta g(A^2 + C^2)} \tag{2}$$

Figure 1. Comparison of broadcast ephemeris errors between CNAV and LNAV (January 2016 - March 2018).
The vertical line separates Block IIR-M satellites (G48-G58) from Block IIF satellites (G62-G73).

where R, A, C represent broadcast orbit errors in radial, along-track and cross-track direc-
tions, respectively; Clk denotes the error of the broadcast clock offset and the weight factors
α and β depend on the altitude of the GNSS satellite. For GPS satellites, these values are
0·98 and 1/49, respectively (Montenbruck et al., 2015).

2.2. *Analysis of CNAV/LNAV broadcast ephemeris error and SISRE.* Broadcast
ephemeris error and SISRE for CNAV and LNAV over a 26-month period from Day 1
in 2016 to Day 62 in 2018 was analysed. IGS precise products of orbit and clock offset
were adopted as a reference by considering the three above-mentioned corrections (Mon-
tenbruck et al., 2018). It should be noted that the SVN G70 and G73 satellites have provided
the CNAV broadcast ephemeris since Day 126 in 2016, for 22 months of the data period.
SISRE outliers exceeding a limit of 15 m were rejected (Steigenberger et al., 2015).

Results of the broadcast ephemeris errors comparison between CNAV and LNAV for
the 19 satellites are shown in Figure 1, which illustrates the Root-Mean-Square (RMS)
of radial, along-track and cross-track orbit errors, as well as that of the clock errors. The
horizontal and vertical axis represents SVN and PRN (Pseudo Random Noise, which cor-
responds to SVN during testing) and errors, respectively in Figure 1. Table 1 presents the
mean RMS of CNAV and LNAV broadcast ephemeris errors for the Block IIR-M and Block
IIF constellations and their mean SISRE.

Compared with LNAV, the orbit error of CNAV is slightly smaller in the radial compo-
nent, but obviously larger errors in the along-track component were observed, which agrees
with the findings in Steigenberger et al. (2015) but improves from 2·23 m to 1·54 m. The
mean RMS of the CNAV clock error for the 19 satellites is almost identical to the LNAV
of no more than 0·5 m, which shows an improvement of around a factor of two compared
to the results in Steigenberger et al. (2015). The improvement is mainly due to the age of
CNAV orbit predictions being changed from three to four days to one day.

The majority of the Block IIF satellites have better accuracy in the clock error than
Block IIR-M. Among all the satellites, however, the accuracy of clock error of two Block

Table 1.   Broadcast ephemeris errors in radial (R), along-track (A) and cross-track (C) directions, and clock errors (T) as well as SISRE for both CNAV and LNAV transmitted by Block IIR-M and Block IIF satellites in a 26-month test period. All values are given in metres.

Component	BLOCK-IIR		BLOCK-IIF		ALL	
	LNAV	CNAV	LNAV	CNAV	LNAV	CNAV
R	0·14	0·13	0·21(0·20)	0·19(0·18)	0·18	0·17
A	1·13	1·65	1·08(1·04)	1·48(1·45)	1·10	1·54
C	0·46	0·45	0·41(0·41)	0·42(0·42)	0·43	0·43
T	0·42	0·42	0·42(0·28)	0·41(0·26)	0·42	0·41
R-T	0·43	0·42	0·49(0·36)	0·46(0·33)	0·47	0·45
SISRE(orb)	0·23	0·28	0·26(0·25)	0·29(0·28)	0·25	0·28
SISRE	0·46	0·49	0·52(0·39)	0·52(0·39)	0·50	0·51

Note: (*) is the mean value for BLOCK-IIF type by excluding G65 and G72.
Orbit-only contributions are indicated by "orb".

IIF satellites of G65 and G72 reaches 1·29 m and 0·98 m, respectively, as they are equipped with caesium clocks. The mean SISRE of all Block IIF satellites is therefore slightly worse than the Block IIR-M satellites. Excluding G65 and G72, mean clock precision and SISRE of all Block IIF satellites reaches 0·26 m and 0·39 m.

CNAV and LNAV SISREs are both at the 0·5 m level, which is further improved in comparison with the results of 0·6 m from 2014 to 2015 published in Steigenberger et al. (2015). SISRE results show that the worse accuracy of the along-track component in satellite orbits does not affect the overall performance of CNAV.

3.   ACCURACY OF CNAV ISC PARAMETERS.

3.1.   *ISC data and update frequency.*   GPS broadcast clock parameters refer to the ionosphere-free linear combination of the L1P(Y) and L2P(Y) pseudorange signals, DCBs have to be considered to correct for systematic effects when carrying out SPP using civil pseudorange observables (Montenbruck and Hauschild, 2013b; Montenbruck et al., 2014). Four additional Inter-Signal Correction (ISC) parameters as a new type of DCB product are introduced in the CNAV message to provide corrections for the legacy L1C/A signal and the new L2C and L5 (L5I5 and L5Q5) signals with respect to L1P(Y), and the detailed definition of ISCs is described in Yin et al. (2014) and Wang et al. (2016a).

Figure 2 shows the updating epochs of TGD and four ISC parameters of CNAV from Day 1 in 2016 to Day 62 in 2018. In Figure 2, the TGDs of the SVN G048, G050, G052, G055 and G062 satellites have never been updated and that of the SVN G053, G057, G063, G064, G065, G067 and G073 satellites were only updated once or twice during the 26 months. The TGDs/ISCs updating frequency of other satellites is relatively higher.

L1C/A ISC, as the only intra-frequency bias parameter, has the lowest update frequency, which has only been updated once for SVN G048, G70 and G73 and twice (that is, day of year (doy) 127 and 160 in 2016) for other satellites. The update frequency of the L2C ISC is higher than TGD and other ISC parameters, where L2C ISC of SVN G066 and G068-072 are updated more than four times. It can be seen that ISCs of L5I5 and L5Q5 of the Block IIF satellites were updated at the same time as the L2C.

The TGD and ISCs of CNAV broadcast ephemerides for the 19 GPS satellites are plotted in Figure 3. Multiple values exist for some parameters of the same satellites, which demonstrate small parameter variations during each updating. Apparent differences are
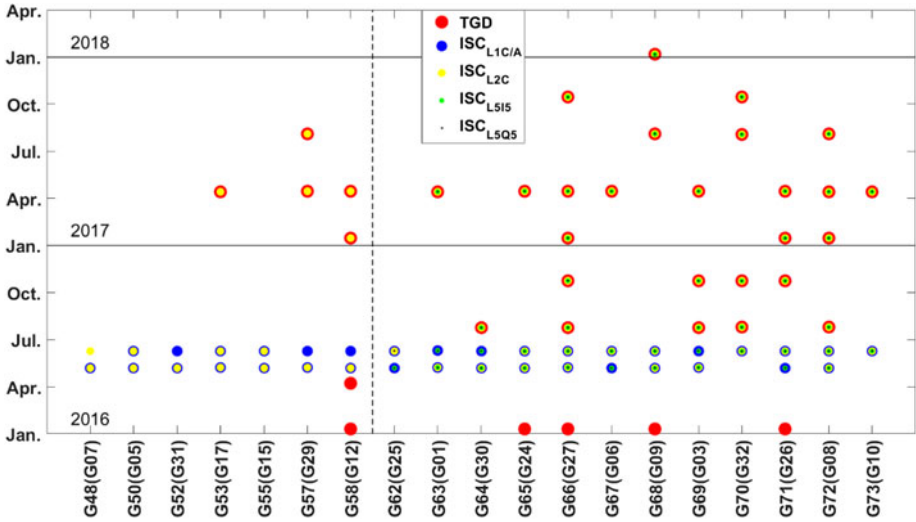
Figure 2.   GPS CNAV broadcast TGD and ISC parameters update time interval. The vertical line separates Block IIR-M satellites (G48-G58) from Block IIF satellites (G62-G73).
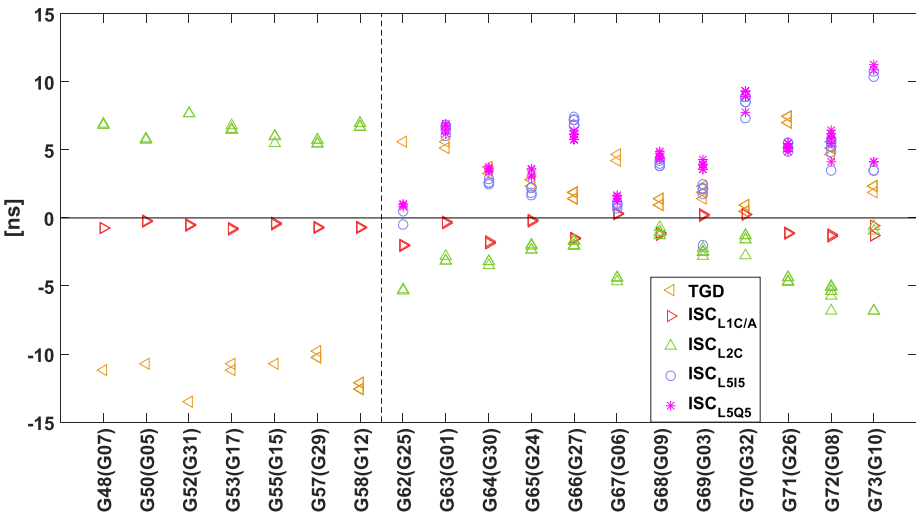

Figure 3.   GPS broadcast TGD and ISC values of each individual satellite (January 2016 − March 2018). The vertical line separates Block IIR-M satellites (G48-G58) from Block IIF satellites (G62-G73). Multiple values exist for some parameters of the same satellites, which demonstrate small parameter variations during each updating.

observed in the TGDs and L2C ISC of Block IIR-M and Block IIF, where they have opposite signs for these two Block types. The L1C/A ISCs have the smallest variation range as they refer to different signals of the same frequency, where the scatter is 2·5 ns for satellites of the Block IIF type and 0·7 ns for the Block IIR-M satellites. On the other hand, the TGD/ISCs of the different Block type satellites show greater differences in comparison with the same Block type satellites, which reaches even more than 20 ns in case of the TGD.
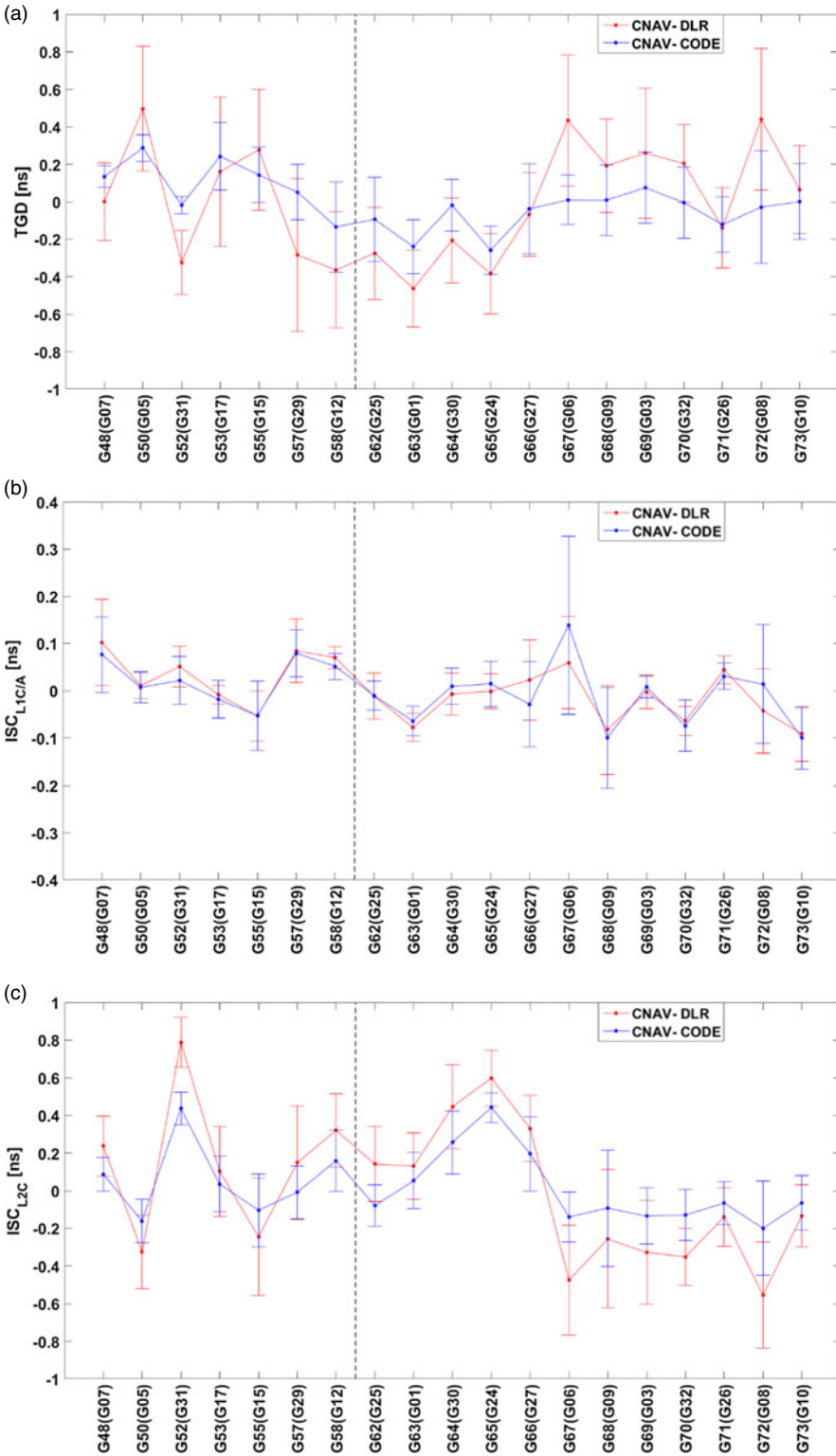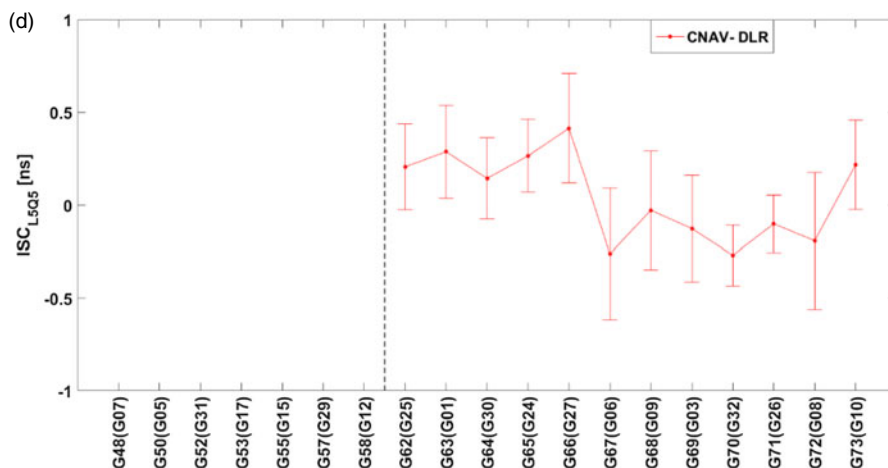
Figure 4.   Continued.

Figure 4.   Mean bias and STD (represented by error bar) of CNAV (a) TGD and (b, c, d) ISCs relative to the DCB products of DLR and CODE. (January 2016 – March 2018). The vertical line separates Block IIR-M satellites (G48-G58) from Block IIF satellites (G62-G73).

Table 2.   Consistency of the CNAV TGD and ISCs relative to that of DLR and CODE. (January 2016 – March 2018). All values are given in nanoseconds.

TYPE	CNAV-DLR		CNAV-CODE	
	Variation	RMS	Variation	RMS
TGD	$-0.46 \sim 0.50$	0.40	$-0.26 \sim 0.29$	0.21
$ISC_{L1C/A}$	$-0.09 \sim 0.10$	0.07	$-0.10 \sim 0.14$	0.08
ISC_{L2C}	$-0.55 \sim 0.79$	0.40	$-0.20 \sim 0.44$	0.23
ISC_{L5Q5}	$-0.27 \sim 0.41$	0.34	—	—

3.2.   *ISC comparison and discussion.*   The accuracy of two different DCB products provided by Deutsches Zentrum für Luft-und Raumfahrtn (DLR) and the Center for Orbit Determination in Europe (CODE) are at the precision of 0·2 ns and 0·1 ns, respectively (Schaer, 2008; Montenbruck et al., 2014; Wang et al., 2016b), which are used as a reference to evaluate the precision of the TGD/ISCs in the CNAV broadcast ephemeris. Table 6 in Steigenberger et al. (2015) lists the detailed relations between TGD/ISCs from the CNAV message and DCBs from DLR and CODE. The TGD and ISCs in CNAV are derived by referring to a calibrated reference receiver at the NGA monitoring station, whereas a zero-mean condition is applied for the DLR and CODE DCBs (Feess et al., 2013; Montenbruck et al., 2014). Considering these different estimation approaches, all values have been re-aligned with the same condition covering the affected satellites, and the detailed realignment method is described in Wang et al. (2016a). More specifically, all Block IIF satellites as reference satellites are selected for constructing a new zero-mean condition since L5 ISCs cannot be provided by Block IIR-M satellites.

Figure 4 and Table 2 show the mean bias and Standard Deviation (STD) of the broadcast TGD and ISCs relative to the DLR and CODE DCBs, respectively. It should be noted that L5I5 ISCs are not presented in Figure 4, because no commercial GNSS receiver could provide observations from the L5I data channel during the validation time period. The mean biases of the CNAV-DLR TGDs vary from −0·46 ns to 0·50 ns, which is obviously

larger than that of the CNAV-CODE TGDs (-0.26 ns ~ 0.29 ns). This may be due to the DLR TGDs being estimated daily, whereas the CODE TGDs represent a monthly average. The agreement of mean L1C/A ISCs between CNAV and DLR/CODE does not exceed 0.14 ns. For the L2C ISCs, mean biases range between $[-0.55$ ns 0.79 ns$]$ and $[-0.20$ ns, 0.44 ns$]$ compared to the DLR and CODE DCBs. The L5Q5 ISCs are compared to DLR DCBs as no such products from CODE were available, and mean biases are in the range $[-0.27$ ns, 0.41 ns$]$.

In general, these results show that the precision of CNAV TGDs and ISCs are about two times worse than those of the DLR/CODE products. Both DLR and CODE use a global tracking network of more than 200 stations, while CNAV data are based on a quite small tracking network of around ten stations (Steigenberger et al., 2015). Although the current CNAV network can provide full global coverage and meet the requirements of real-time processing, the accuracy of CNAV TGDs and ISCs could be further improved if more stations were added.

4. PERFORMANCE OF CNAV/LNAV BROADCAST EPHEMERIS ON GPS STANDARD POSITIONING.

4.1. *Test data and processing strategy.*   To further assess the performance of CNAV, we apply the CNAV/LNAV for SPP in different scenarios. 22 MGEX stations shown in Figure 5 and a 30-day period of Day 70 to Day 99 in 2018 was selected. A Hatch filter was applied to smooth the pseudo-range to reduce the impact of the code noise (Hatch, 1982; Chang et al., 2015). Other SPP process settings were as follows: the orbits and clocks from broadcast ephemeris; the ionosphere-free linear combination of P code observations at a sampling rate of 30 s was used for dual-frequency SPP with a cut-off angle of $10°$; a Global Ionosphere Map (GIM) model was applied to correct the ionospheric error for single-frequency SPP (Schaer and Werner, 1998; Jee et al., 2010); tropospheric errors were corrected by the GPT2w model (Böhm et al., 2015), and the coordinates and receiver clocks were estimated epoch by epoch in a Kalman filter.

As only 12 GPS Block IIF satellites transmitted L5Q signals during the validation time period, we utilised the P code observables C1C, C2L, C1W and C2W of the 19 GPS satellites for positioning and specific scenarios are as follows:

(1) C1C/C1W and C2L/C2W-based kinematic single-frequency SPP using the broadcast ephemeris of LNAV-only, CNAV-only and CNAV + ISC, where LNAV-only and CNAV-only mean using satellite orbits/clocks from LNAV and CNAV without consideration of ISC, and CNAV + ISC refers to the use of satellite orbits/clocks of CNAV together with an ISC parameter. Since there are no ISCs for C1W and C2W, C1W and C2W-based SPP using LNAV-only and CNAV-only are compared.

The pseudo-range observation equations with and without the consideration of ISCs on the L1 and L2 frequency can be expressed as:

$$\left.\begin{array}{l} P^s_{r,f_1} = \rho^s_r + c \cdot (dT_r - dT^s) + c \cdot TGD + dTrop + \lambda_1 \cdot dIon + \varepsilon_P \\ P^s_{r,f_1} = \rho^s_r + c \cdot (dT_r - dT^s) + c \cdot TGD - c \cdot ISC_{L1C/A} + dTrop + \lambda_1 \cdot dIon + \varepsilon_P \end{array}\right\} \quad (3)$$

$$\left.\begin{array}{l} P^s_{r,f_2} = \rho^s_r + c \cdot (dT_r - dT^s) + c \cdot (f_1/f_2)^2 \cdot TGD + dTrop + \lambda_2 \cdot dIon + \varepsilon_P \\ P^s_{r,f_2} = \rho^s_r + c \cdot (dT_r - dT^s) + c \cdot TGD - c \cdot ISC_{L2C} + dTrop + \lambda_2 \cdot dIon + \varepsilon_P \end{array}\right\} \quad (4)$$

where P^s_{r,f_1}, P^s_{r,f_2} are the pseudo-range observations on the L1 and L2 frequencies, respectively; ρ^s_r is the geometric range between the receiver and satellites; dT_r and dT^s are
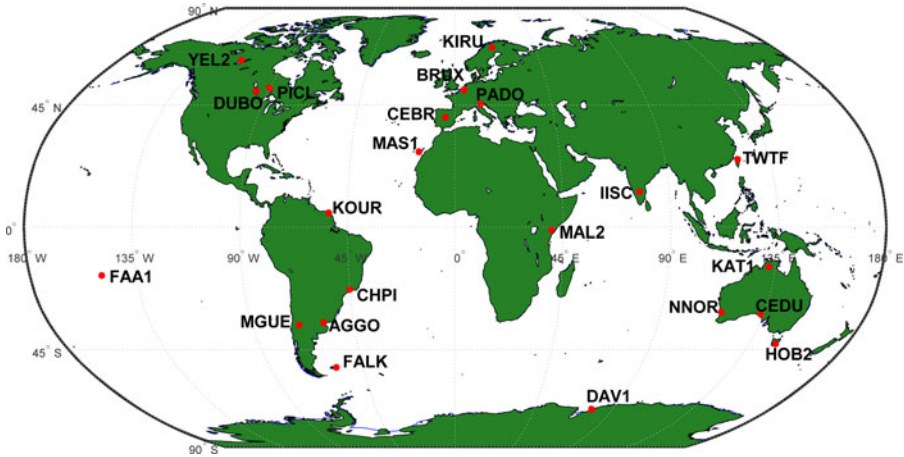
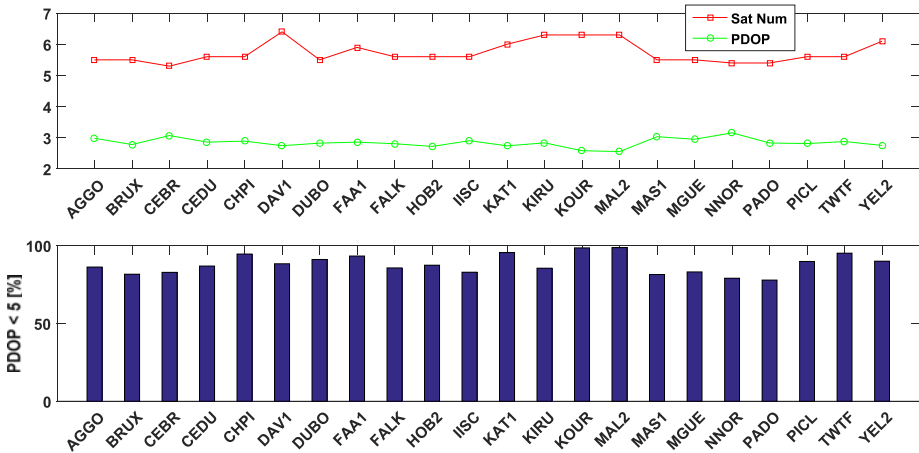Figure 5.   Distribution of the selected 22 MGEX stations.

Figure 6.   Mean of PDOP, visible satellites number and the percentage of PDOP less than 5·0 for 22 MGEX stations.

the receiver and satellite clock bias, respectively; $dTrop$ is the slant tropospheric delay, $\lambda_i = 40 \cdot 28/f_i^2$ $(i = 1, 2)$ and $\lambda_i \cdot dIon$ is the slant ionospheric delay; c is light speed and ε_P is a noise term.

(2) C1C/C2L ionosphere-free combination-based kinematic dual-frequency SPP using the broadcast ephemeris of LNAV-only, CNAV-only and CNAV + ISC, respectively.

The dual-frequency pseudo-range observation equations with and without the consideration of ISCs can be expressed as

$$\left. \begin{aligned} P_{r,IF}^s &= \rho_r^s + c \cdot (dT_r - dT^s) + dTrop + \varepsilon_P \\ P_{r,IF}^s &= \rho_r^s + c \cdot (dT_r - dT^s) + c \cdot TGD - c \cdot \frac{ISC_{L2C} - (f_1/f_2)^2 \cdot ISC_{L1C/A}}{1 - (f_1/f_2)^2} + dTrop + \varepsilon_P \end{aligned} \right\} \tag{5}$$
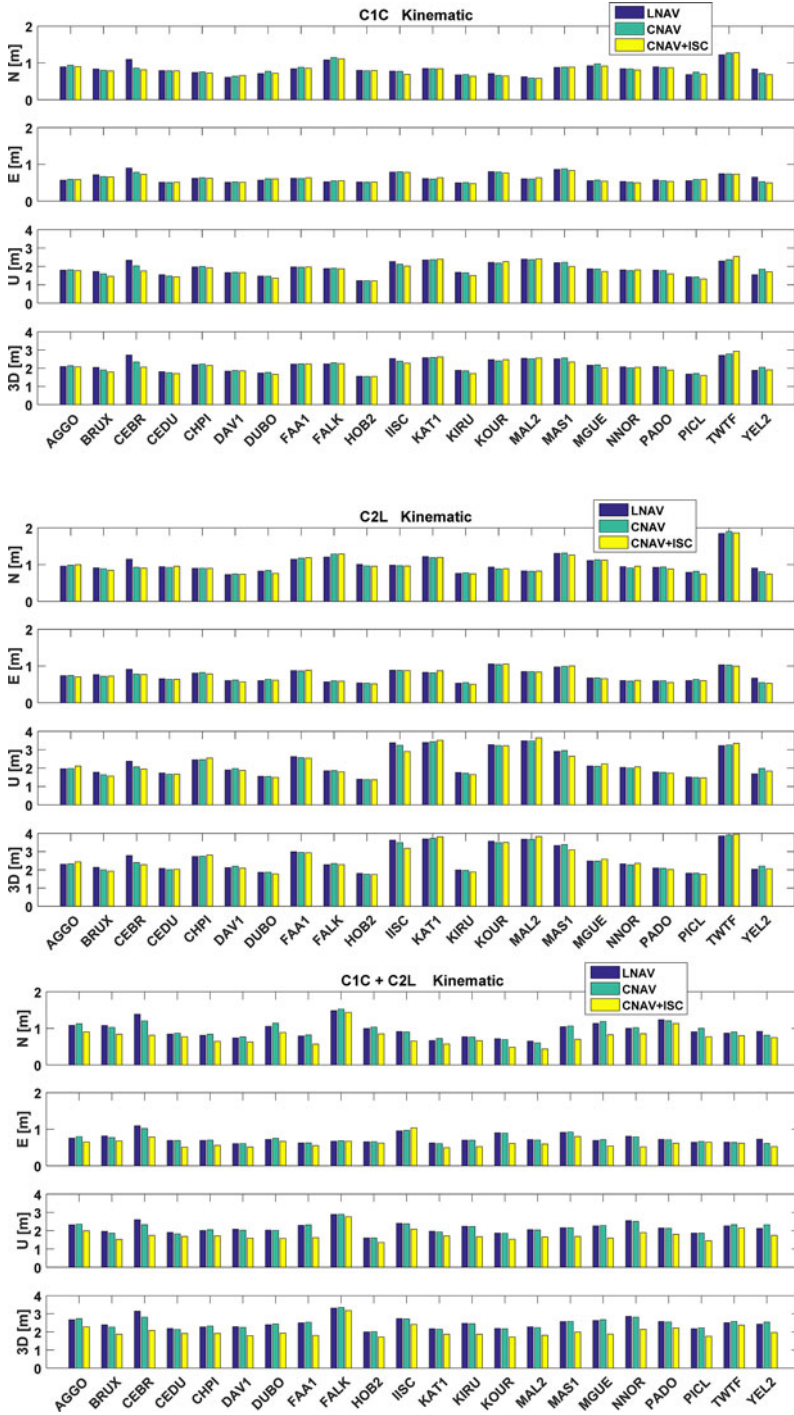
Figure 7.   RMS of positioning errors in north-south, east-west, up and 3D components for 22 MGEX stations in different SPP schemes.

Table 3.   RMS of positioning errors in different SPP schemes. All values are given in metres.

| | Kinematic | | | | | | | | |
| | Vertical | | | Horizontal | | | 3D | | |
Type	LNAV	CNAV	CNAV + ISC	LNAV	CNAV	CNAV + ISC	LNAV	CNAV	CNAV + ISC
C1C	1·89	1·87	1·81	1·05	1·04	1·02	2·16	2·14	2·08
C1W	1·80	1·78	—	1·01	1·00	—	2·07	2·05	—
C2L	2·28	2·26	2·23	1·26	1·25	1·23	2·62	2·59	2·56
C2W	2·23	2·21	—	1·22	1·21	—	2·56	2·53	—
C1C + C2L	2·17	2·15	1·75	1·22	1·22	1·00	2·49	2·48	2·02
C1W + C2W	1·68	1·65	—	0·96	0·95	—	1·94	1·91	—

(3) Dual-frequency SPP based on the C1C/C2L ionosphere-free combination (using broadcast ephemeris of CNAV + ISC) and dual-frequency SPP based on the C1W/C2W ionosphere-free combination using the broadcast ephemeris of LNAV-only and CNAV-only.

4.2.   *Precision analysis of GPS SPP with and without ISCs.*   Using the 19 satellites only, the upper subgraph in Figure 6 shows the average number of visible satellites and mean Position Dilution of Precision (PDOP) in a daily SPP solution for selected MGEX stations. The lower subgraph in Figure 6 gives the percentage of epochs with PDOP less than 5·0 in the total epochs of one day for each station. An average of five to seven satellites could be observed at each station, but most of these stations had less than six satellites in view. The mean PDOP varied from 2·6 to 3·1 and the percentage of healthy epochs (PDOP < 5) was from 77·8% to 98·6% for all stations; only one third of the total stations exceeded 90%.

Figure 7 shows the RMS of SPP positioning errors under the above-mentioned different scenarios for the 22 MGEX stations in the test period, and mean RMS of single- and dual-frequency SPP positioning errors in the horizontal, vertical and Three-Dimensional (3D) components are described in Table 3.

C1C/C1W and C2L/C2W-based single-frequency SPP based on LNAV-only/CNAV-only achieves the same precision as that of single-frequency SPP with the consideration of ISCs using CNAV + ISC. C1C/C1W-based single-frequency SPP has a precision of about 2·1 m in 3D and that of C2L/C2W is a little bit worse at around 2·6 m, due to a relatively larger range of noise.

C1C/C2L ionosphere-free combination-based dual-frequency SPP without ISC correction exhibits RMS of 1·22 m and 2·15 m in horizontal and vertical components, respectively. Considering the ISCs results in smaller positioning errors with RMS of 1·00 m in the horizontal direction and 1·75 m in the vertical and 3D RMS was improved by about 18·6%. More interestingly, the C1W/C2W ionosphere-free combination-based dual-frequency SPP under scenario 3, where no ISCs corrections were applied, achieved the best precision among all scenarios. Its position RMS is less than 1·00 m and 1·70 m in horizontal and vertical directions, respectively. This implies that the ISCs of C1W and C2W may be quite close and thus they have little impact on SPP.

5. CONCLUSIONS.   Compared with LNAV, CNAV provides a different type of encoding mechanism and more flexible message structures, as well as benefitting from a large

number of orbit parameters, which aim at producing a substantially smoother and more precise broadcast orbit. In addition, the new DCB information such as the ISCs for users of the civil signals is introduced in the CNAV to correct for systematic effects depending on the used signals and frequencies. This paper selects the CNAV/LNAV broadcast ephemeris and IGS precise GPS products from the period from January 2016 to March 2018 to evaluate the CNAV/LNAV performance, including precision of orbits, clocks, SISREs and SPP.

The performance of CNAV broadcast ephemeris is essentially identical to the LNAV for the same satellites. The CNAV/LNAV SISRE and SISRE(orb) from January 2016 to March 2018 amounts to roughly 0·5 m and 0·3 m, respectively, which is further improved in comparison with the results from 2014 to 2015. The SISRE of Block IIF satellites (excluding G65 and G72) is around 0·1 m lower than that of IIR-M satellites.

The L1C/A ISC parameter has the lowest update frequency among all ISCs and they are updated no more than twice in a 26-month period. For the different Block types, the TGDs/ISCs update frequency of the Block IIF satellites is significantly higher than that of Block IIR-M satellites.

The agreement of the TGDs/ISCs with DLR and CODE DCB products is slightly different, where the precision of L1C/A ISCs is better than 0·1 ns and those of the TGD, L2C ISCs and L5Q5 ISCs are about 0·4 ns.

ISC correction has little effect on single-frequency SPP for GPS users using civil signals (for example, L1C, L2C), whereas application of these ISCs in dual-frequency SPP using C1C + CL2 observations results in positioning errors with an RMS of 1·00 m in the horizontal direction and 1·75 m in the vertical direction and 3D RMS was improved by about 18·6%. The C1W/C2W ionosphere-free combination-based dual-frequency SPP without ISC corrections achieves the best precision among all scenarios. Its position RMS is less than 1·00 m and 1·7 m in horizontal and vertical directions, respectively, which implies that the ISCs of C1W and C2W may be quite close, and thus they have little impact on SPP.

ACKNOWLEDGEMENTS

REFERENCES

Böhm, J., Möller, G., Schindelegger, M., Pain, G. and Weber, R. (2015). Development of an improved empirical model for slant delays in the troposphere (GPT2w). *GPS Solutions*, **19**, 433–441.

Chang, Z.Q., Hu, X.G., Guo, R., Cao, Y.L., Wu, X.L., Wang, A.B. and Dong, E.Q. (2015). Comparison between CNMC and hatch filter & its precision analysis for BDS precise relative positioning. *Scientia Sinica Physica, Mechanica & Astronomica*, **45**, 079508.

Cohenour, C. and Van Graas, F. (2011). GPS orbit and clock error distributions. *Navigation*. **58**, 17–28.

Creel, T., Dorsey, A.J., Mendicki, P.J., Little, J., Mach, R.G. and Renfro, B.A. (2007). Summary of accuracy improvements from the GPS legacy accuracy improvement initiative(L-AII). *Proceedings of ION GNSS*, 2481–2498.

Du, L., Liu, Z.J., Zhou, P.Y., Fang, S.C., Liu, L. and Ma, G.F. (2017). GEO NAV/CNAV-type broadcast ephemeris fitting without rotation of inclination. *Acta Geodaetica et Cartographica Sinica*, **46**, 297–306.

Feess, W., Cox, J., Howard, E. and Kovach, K. (2013). GPS inter-in-signal corrections (ISCs) study. *In Proceedings of the 26th International Technical Meeting of the Satellite Division of the Institute of Navigation (ION GNSS+ 2013), Nashville, TN*, 951–958.

Hatch, R.R. (1982). The synergism of GPS code and carrier measurements. *Proceedings of the 3th International Geodetic Symposium on Satellite Doppler Positioning, New Mexico*, 1213–1232.

Heng, L., Gao G.X., Walter, T and Enge, P. (2011). Statistical characterization of GPS signal-in-space errors. *Proceedings of ION ITM 2011, San Diego, CA*, 312–319.

Hofmann-Wellenhof, B., Lichtenegger, H. and Wasle, E. (2008). GNSS-Global Navigation Satellite Systems: GPS, GLONASS, Galileo, and more. *Springer-Verlag Vienna*.

IS-GPS-200H. (2014). Interface specification IS-GPS-200: navstar GPS space segment/navigation user segment interfaces. *Technical Report Global Positioning System Directorate Systems Engineering & Integration*. Available: http://www.gps.gov/technical/icwg/IS-GPS-200H.pdf.

IS-GPS-705D. (2014). Interface specification IS-GPS-705: navstar GPS space segment/user segment L5 interfaces. *Technical Report Global Positioning System Directorate Systems Engineering & Integration*. Available: http://www.gps.gov/technical/icwg/IS-GPS-705D.pdf.

Jee, G., Lee, H.B., Kim, Y.H., Chung, J.K. and Cho, J. (2010). Assessment of GPS global ionosphere maps (GIM) by comparison between CODE GIM and TOPEX/Jason TEC data: ionospheric perspective. *Journal of Geophysical Research*, **115**, A10319.

Montenbruck, O. and Hauschild, A. (2013). Code biases in multi-GNSS point positioning. *In Proceedings of the 2013 International Technical Meeting of the Institute of Navigation, San Diego, CA*, 616–628.

Montenbruck, O., Hauschild, A. and Steigenberger, P. (2014). Differential code bias estimation using multi-GNSS observations and global ionosphere maps. *Navigation*, **61**, 191–201.

Montenbruck, O., Langley, R.B. and Steigenberger, P. (2013). First live broadcast of GPS CNAV message. *GPS World*, **24**, 14.

Montenbruck, O., Steigenberger, P. and Hauschild, A. (2015). Broadcast versus precise ephemerides: a multi-GNSS prespective. *GPS solutions*, **19**, 321–333.

Montenbruck, O., Steigenberger, P. and Hauschild, A. (2018). Multi-GNSS signal-in-space range error assessment – methology and results. *Advances in Space Research*, **03**, 041.

Petit, G. and Luzum, B. (2010). IERS Conventions. *IERS Technical 2010 Note 36*. Verlag des Bundesamts für Kartographie und Geodäsie, Frankfurt am Main, Germany. 2010.

Schaer, S. (2008). Differential code biases (DCB) in GNSS analysis. *In Proceedings of IGS Workshop 2008, Miami Beach: Swiss Federal Office of Topography Swisstopo*.

Schaer, S. and Werner, G. (1998). How to use IONEX. *igscb.jpl.nasa.gov/igscb/data/format/ionex1.pdf*.

Schmid, R., Steigenberger, P., Gendt, G., Ge, M. and Rothacher, M. (2007). Generation of a consistent absolute phase-center correction model for GPS receiver and satellite antennas. *Journal of Geodesy*, **81**, 781–798.

Steigenberger, P., Montenbruck, O. and Hessels, U. (2015). Performance evaluation of the early CNAV navigation message. *Proceedings of the 2015 International Technical Meeting of the Institute of Navigation, Dana Point, California*, 155–163.

Wang, L.X., Huang, Z.G, and Zhao, Y. (2014). Navigation message designing with high accuracy for NAV. *Chinese Journal of Aeronautics*, **27**, 994–1001.

Wang, N.B., Yuan, Y.B., Li, Z.S., Montenbruck, O. and Tan, B.F. (2016b). Determination of differential code biases with multi-GNSS observations. *Journal of Geodesy*, **90**, 209–228.

Wang, N.B., Yuan, Y.B., Zhang, B.C. and Li, Z.S. (2016a). Accuracy evaluation of GPS broadcast Inter-signal Correction(ISC) parameters and their impacts on GPS standard positioning. *Acta Geodaetica et Cartographica Sinica*, **45**, 919–928.

Warren, D.L. and Raquet, J.F. (2003). Broadcast vs. precise GPS ephemerides: a historical perspective. *GPS Solutions*, **7**, 151–156.

Yin, H., Morton, Y., Carroll, M. and Vinande, E. (2014). Performance analysis of L2 and L5 CNAV broadcast ephemeris for orbit calculation. *In Proceedings of the 2014 International Technical Meeting of the Institute of Navigation, San Diego, CA*, 761–768.

Zhang, Y.Z., Chen, J.P., Zhou, J.H., Yang, S.N., Wang, B., Chen, Q. and Gong, X.Q. (2016). Analysis and Application of BDS broadcast ephemeris Bias. *Acta Geodaetica et Cartographica Sinica*, **45**, 64–71.